Synthesis of perovskite-type oxynitrides $SrNb(O,N)_3$ and $CaTa(O,N)_3$ using carbon nitride

Qian Yang[1], Yuji Masubuchi[2*], Mikio Higuchi[2]

[1] Graduate School of Information Science and Technology, Hokkaido University, N14W9, Kita-ku, Sapporo 060−0814, Japan.

[2]Faculty of Engineering, Hokkaido University, N13W8, Kita-ku, Sapporo 060-8628, Japan.

Corresponding Author

* Yuji Masubuchi; address: Faculty of Engineering, Hokkaido University, N13 W8, Kita-ku, Sapporo, 060-8628, Japan; TEL/FAX:+81-(0)11-706-6742/6739; E-mail: yuji-mas@eng.hokudai.ac.jp

Abstract

The synthesis of oxynitride perovskites based on the use of gaseous ammonia as the nitrogen source requires high reaction temperatures and long durations. In the resent work, reduction and nitridation reactions using carbon nitride (C_3N_4) were employed to prepare $SrNbO_2N$ and $CaTaO_2N$ from their oxide precursors, without the use of ammonia. The phase evolution behaviors and the reaction mechanisms were investigated by acquiring thermogravimetric and X-ray diffraction data. The formation of metal cyanamide as an

intermediate was found to be vital to realizing low-temperature synthesis of these compounds. Scanning electron microscopy observations also indicated that the particle sizes of the oxynitrides prepared using C_3N_4 were smaller than those obtained by ammonolysis reactions, due to the low formation temperature of 800 °C associated with the present C_3N_4 process.

Key words: perovskite; oxynitrides; carbon nitride; powder processing

Introduction

Perovskite oxynitrides having the general formulae ABO_2N and $ABON_2$ are useful functional materials with a wide range of applications. The majority of known perovskite-type oxynitrides have potential applications as dielectric materials [1], photocatalysts [2, 3] and nontoxic pigments [4]. The conventional preparation route for oxynitrides is the thermal ammonolysis of oxides under a flow of gaseous ammonia. However, a high reaction temperature and long duration are required for the ammonolysis reaction due to the limited diffusion rate of nitrogen [1, 5]. In order to overcome these extreme aspect of processing, several novel synthesis approaches that do not use ammonia have been investigated. Sun et al. developed a direct synthesis approach for the oxynitride $SrTaO_2N$ from $SrCO_3$ and Ta_3N_5 in a nitrogen atmosphere [6]. Clark et al. reported that $ATaO_2N$ (A=Ca, Ba, Sr) could be synthesized through a high-temperature solid-state reaction between AO and TaON at 1500 °C for 3 h under N_2 [7]. However, prior to this heat-

treatment, the Ta_3N_5 and TaON must be produced by heating Ta_2O_5 under a flow of ammonia at 950 and 850 °C, respectively. The utilization of ammonia is thus not avoided in these processing routes. In our own previous work, we successfully synthesized $SrTaO_2N$ using carbon nitride (C_3N_4) [8]. In this process, the C_3N_4 reacts with the $Sr_2Ta_2O_7$ precursor to form $SrCN_2$ and Ta_3N_5 intermediates on residual $Sr_2Ta_2O_7$. These intermediates then react with the oxide residue to form $SrTaO_2N$ at 800 °C, which is 200 °C lower than the temperature required for ammonolysis. Recently, the formation of metal cyanamide (*M*-CN_2) intermediates, such as $La_2O_2CN_2$ and $ZnCN_2$ has also been suggested as an ammonia-free synthesis of the oxynitrides $LaTiO_2N$ and GaN:ZnO, respectively [9, 10]. It is evident that intermediates play an important role in the formation of oxynitrides in these systems, although the reactivity of C_3N_4 with other oxide precursors to form perovskite-type oxynitrides has not yet been examined. Metal cyanamides can be obtained from many alkaline and alkaline earth metals and, in the present work, we used $Sr_2Nb_2O_7$ or $Ca_2Ta_2O_7$ as precursors for nitridation reactions with C_3N_4 to synthesize $SrNbO_2N$ and $CaTaO_2N$, respectively. The reactivity of C_3N_4 with the precursors to form oxynitride perovskites was investigated by comparing the formation of intermediate phases.

Experimental procedure

The oxide precursors were prepared from the raw materials $CaCO_3$ (purity 99.9%, Fujifilm Wako Pure Chemical Co.), $SrCO_3$ (purity 99.9%, Fujifilm Wako Pure Chemical

Co.), Ta_2O_5 (purity 99.9%, Fujifilm Wako Pure Chemical Co.) and Nb_2O_5 (purity 99.9%, Fujifilm Wako Pure Chemical Co.). Stoichiometric mixtures of the carbonates and oxides were calcined at 1200 °C for 10 h in air to prepare the $Sr_2Nb_2O_7$ and $Ca_2Ta_2O_7$ precursors. The mixtures were ground and calcined twice to obtain phase-pure oxide precursors. C_3N_4 was synthesized via the calcination of melamine (purity 99.0%, Fujifilm Wako Pure Chemical Co.) at 550 °C for 6 h in air. A small amount of hydrogen remained in the calcined product and the chemical composition of the product was estimated to be $C_3N_{4.5}H_{1.5}$ based on CHN analysis, although the compound is still referred to herein as C_3N_4. The oxide precursors were mixed with the C_3N_4 by ball milling using zirconia balls and ethanol, employing a $Sr_2Nb_2O_7$ or $(Ca_2Ta_2O_7)$:C_3N_4 molar ratio of 1:1.5. Each mixture was subsequently pressed into a pellet and then loaded into an alumina boat, after which it was heated at various temperatures for 6 h in a N_2 flow (50 ml/min, 99.99%) in a silica tube furnace.

The crystalline phases of the products were determined by powder X-ray diffraction (XRD; Ultima IV, Rigaku), collecting data at 0.02° steps over the 2θ range of 15° to 60°. Thermogravimetric differential thermal analysis (TG-TGA) data were acquired using a thermogravimetric analyzer (STA 2500, NETZSCH) in a nitrogen flow of 100 ml/min. The sample chamber was evacuated to 10 Pa prior to the measurements. The morphology of each product was observed by field-emission scanning electron microscopy (FE-SEM, JSM-6500F, JEOL).

Results and discussion

The thermal behavior of a $Sr_2Nb_2O_7/C_3N_4$ mixture was examined using TGA under a flow of nitrogen. The resulting TGA plot (Figure 1) exhibits three stages. The first significant mass loss of 21.5% started at 380 °C and finished at approximately 700 °C, while the second loss of 2.1% occurred around 800 °C. The TGA curve was almost constant above 1000 °C after the third mass loss. XRD patterns were obtained at each final temperature associated with a mass loss and are shown in Figure 2. Only diffraction peaks attributed to $Sr_2Nb_2O_7$ present in the pattern for the starting mixture (Figure 2(a)) because of the amorphous nature of the C_3N_4. At 700 °C, a small amount of $SrCN_2$ and a niobium-based rock salt phase can be observed together with residual $Sr_2Nb_2O_7$. A $Sr_4Nb_2O_9$ impurity was formed along with the perovskite phase and the rock salt phase at 1100 °C. The oxygen and nitrogen concentrations in the perovskite phase could not be accurately determined because of the presence of the minor impurity phases. Hence, hereafter, the chemical formula the perovskite phase is denoted as $SrNb(O,N)_3$. The TGA and XRD results suggest that the first and largest mass loss was caused by the decomposition of C_3N_4 as shown in Figure S1 in Supporting Information (SI) together with the formation of SrCN2 and rock salt type Nb(O,N). The generation of the perovskite phase from $SrCN_2$, Nb(O,N) and unreacted $Sr_2Nb_2O_7$ caused the second mass loss, similar to results obtained during $SrTaO_2N$ formation from $Sr_2Ta_2O_7$ and C_3N_4 [8]. The third mass loss is ascribed to the decomposition of the perovskite phase, in which the $SrNb(O,N)_3$ decomposed to $Sr_4Nb_2O_9$ and a rock salt phase. The thermal decomposition of the $SrNbO_2N$ was

investigated in an Ar flow and this material was determined to degrade to give a mixture of $Sr_4Nb_2O_9$ and the rock salt-like compound Nb_4N_3 together with significant N_2 release above 950 °C [11].

The mixture of $Sr_2Nb_2O_7/C_3N_4$ was also heated at temperatures from 600 to 800 °C for 6 h in the tube furnace under a flow of N_2, and the XRD patterns obtained from the products are shown in Figure S2 in the SI. At 600 °C, a small amount of $SrCN_2$ and a rock salt phase were observed together with $Sr_2Nb_2O_7$, in agreement with the TGA results. At 700 °C, the perovskite phase appeared along with $SrCN_2$ and rock salt phase intermediates, although a portion of the $Sr_2Nb_2O_7$ still remained. A nearly pure $SrNb(O,N)_3$ perovskite phase with only a small quantity of a minor phase was obtained at 800 °C. The formation of the $SrNb(O,N)_3$ perovskite could therefore be achieved at temperatures as low as 800 °C in a flow of N_2, rather than at the temperature of 950 °C required for NH_3-based nitridation [12]. The products appeared black, suggesting the presence of an electrically conductive impurity such as a rock salt-type niobium phase as shown in Fig. S3 in the SI. The lattice parameters for the product were determined to be a = 5.70756(3) Å, c = 8.09421(1) Å and c/√2a = 1.00278Å, all of which are smaller than the literature values (a = 5.71068(3) Å, c = 8.10400(7) Å, c/√2a value = 1.0034 Å) [12]. The smaller lattice parameters and c/√2a value are attributed to partial nitrogen loss from the perovskite-type oxynitride, as has also been reported in the case of the nitrogen deficient compound $SrTaO_2N_{0.7}$ [13]. This partial nitrogen loss indicates that the perovskite phase was electrically conductive due to the reduction of Nb. The black color can also be ascribed

to the presence of an electrically conductive perovskite phase. In comparison, calcination reactions of mixtures with the $Sr_2Nb_2O_7$:C_3N_4 molar ratios of 1:1 and 1:2 were conducted at the same heating conditions. Insufficient and over-reduction reactions were observed at molar ratios of 1:1 and 1:2, respectively as shown in Fig. S4 in the SI.

The TGA results obtained from the $Ca_2Ta_2O_7$/C_3N_4 mixture are presented in Figure 3. A significant mass loss of 16.2% occurred between 380 and 750 °C, after which a second mass loss of 2.6% is evident. The XRD patterns for the TGA samples at the temperatures associated with each mass loss are shown in Figure 4. At 750 °C, the diffraction pattern did not change from that for the oxide precursor and, even at 1100 °C, the oxide precursor still remained together with the perovskite-type $CaTa(O,N)_3$ phase. Characteristic diffraction lines for $CaCN_2$ were not observed at any point.

The XRD pattern for the material obtained from the nitridation of $Ca_2Ta_2O_7$ at 800 °C in the tube furnace for 6 h is shown in Figure S5 in the SI. A part of the original $Ca_2Ta_2O_7$ remained in the specimen produced after heating at 800 °C, together with the $CaTa(O,N)_3$ perovskite, and so the product was mixed with C_3N_4 again to conduct a second heat treatment. The residual $Ca_2Ta_2O_7$ disappeared after the second heating, while Ta_3N_5 and TaN were formed. The product had a dark green coloration as shown in Fig. S6 in the SI, implying that over-reduction had been caused by the additional C_3N_4. We also conducted a calcination of a mixture of $Ca_2Ta_2O_7$:C_3N_4 with a molar ratio of 1:3. XRD pattern of the product is shown in Fig. S7. By increasing the molar ratio of C_3N_4, large amount of $Ca_2Ta_2O_7$ remained and an impurity phase of Ta_3N_5 appeared. Compared with this result,

a second heat treatment with additional C_3N_4 is an efficient way to enhance the phase purity of $CaTa(O,N)_3$. In previous work, $SrTaO_2N$ was obtained from the reaction between the intermediates $SrCN_2$ and Ta_3N_5 and residual $Sr_2Ta_2O_7$ in an one-step process [8]. The lack of formation of $CaCN_2$ during this process might therefore necessitate a two-step heat treatment to consume the starting $Ca_2Ta_2O_7$ and to obtain $CaTa(O,N)_3$.

The $SrCN_2$ intermediate was detected as an intermediate following the reaction between $Sr_2Nb_2O_7$ and C_3N_4, and reacted with the rock salt phase and the residual oxide precursor to produce $SrNb(O,N)_3$, similar to the case of $SrTaO_2N$ [8]. In contrast, the absence of $CaCN_2$ indicates that the reaction mechanism associated with a $Ca_2Ta_2O_7/C_3N_4$ mixture is different from that for a $Sr_2Nb_2O_7/C_3N_4$ mixture. In some studies, $SrCN_2$ has been obtained from $SrCO_3$ by heating in a flow of gaseous ammonia at 700 °C. However, the synthesis of phase-pure $CaCN_2$ from $CaCO_3$ under ammonia is challenging, suggesting that the formation of $CaCN_2$ is more difficult than that of $SrCN_2$ [14-16]. Because of the presence of $SrCN_2$ as an intermediate, the perovskite phase could be obtained at 800 °C when synthesizing $SrTaO_2N$ [8] and $SrNb(O,N)_3$. Conversely, in the case of $CaTa(O,N)_3$, the absence of $CaCN_2$ required the addition of C_3N_4 to achieve the nitridation of the residual $Ca_2Ta_2O_7$.

The morphologies of these specimens were examined using FE-SEM, as shown in Figure 5. The particle size of approximately 100 nm was smaller than that for material produced via the ammonolysis method. These smaller particles resulted from the lower formation temperature, and would be suitable for photocatalysis applications and as precursors for

sintering.

Conclusion

Nearly pure single phases of $SrNb(O,N)_3$ and $CaTa(O,N)_3$ were obtained from $Sr_2Nb_2O_7/C_3N_4$ and $Ca_2Ta_2O_7/C_3N_4$ mixtures, respectively. Reactions between intermediates and the unreacted oxide precursor formed the perovskite phase $SrNb(O,N)_3$ at a lower reaction temperature and in a shorter reaction time as compared to the ammonia nitridation method. It was determined that the lack of formation of $CaCN_2$ during the reaction between $Ca_2Ta_2O_7$ and C_3N_4 requires a two-step heat treatment to obtain $CaTa(O,N)_3$. The particle sizes of the samples prepared using C_3N_4 were significantly smaller than those derived from the ammonolysis reaction.

Acknowledgements

This work was supported by Grants-in-Aid for Scientific Research on Innovative Areas, “Mixed Anion” (nos. JP16H06438 and JP16H06439) from the Japan Society for the Promotion of Science (JSPS).

References

[1] Y. Masubuchi, S.-K. Sun, S. Kikkawa, Processing of dielectric oxynitride perovskites for powders, ceramics, compacts and thin films, Dalton Trans. 44 (2015) 10570-10581.

[2] K. Maeda, K. Domen, New non-oxide photocatalysts designed for overall water splitting under visible light, J. Phys. Chem. C. 111 (2007) 7851-7861.

[3] S.G. Ebbinghaus, H.-P. Abicht, R. Dronskowski, T. Müller, A. Reller, A. Weidenkaff, Perovskite-related oxynitrides–recent developments in synthesis, characterisation and investigations of physical properties, Prog. Solid State Chem. 37 (2009) 173-205.

[4] M. Jansen, H.-P. Letschert, Inorganic yellow-red pigments without toxic metals, Nat. 404 (2000) 980.

[5] T. Motohashi, Y. Hamade, Y. Masubuchi, T. Takeda, K.-i. Murai, A. Yoshiasa, S. Kikkawa, Structural phase transition in the perovskite-type tantalum oxynitrides, $Ca_{1-x}EuxTa\ (O, N)_3$, Mater. Res. Bull. 44 (2009) 1899-1905.

[6] S.-K. Sun, T. Motohashi, Y. Masubuchi, S. Kikkawa, Direct synthesis of $SrTaO_2N$ from $SrCO_3/Ta_3N_5$ involving CO evolution, J. Eur. Ceram. Soc. 34 (2014) 4451-4455.

[7] S.J. Clarke, K.A. Hardstone, C.W. Michie, M.J. Rosseinsky, High-temperature synthesis and structures of perovskite and n= 1 Ruddlesden− Popper tantalum oxynitrides, Chem. Mater. 14 (2002) 2664-2669.

[8] Y. Masubuchi, M. Tadaki, S. Kikkawa, Synthesis of the perovskite $SrTaO_2N$ using C_3N_4 for both reduction and nitridation, Chem. Lett. 47 (2017) 31-33.

[9] R. Okada, K. Katagiri, Y. Masubuchi, K. Inumaru, Preparation of $LaTiO_2N$ using hydrothermally synthesized $La_2Ti_2O_7$ as a precursor and urea as a nitriding agent, Eur. J. Inorg. Chem. 2019 (2019) 1257-1264.

[10] K. Katagiri, Y. Hayashi, R. Yoshiyuki, K. Inumaru, T. Uchiyama, N. Nagata, Y. Uchimoto, A. Miyoshi, K. Maeda, Mechanistic insight on the formation of GaN: ZnO solid solution from Zn-Ga layered double hydroxide using urea as the nitriding agent,

Inorg. Chem. 57 (2018) 13953-13962.

[11] R. Aguiar, D. Logvinovich, A. Weidenkaff, A. Reller, S.G. Ebbinghaus, Thermal oxidation of oxynitride perovskites in different atmospheres, Thermochim. Acta 471 (2008) 55-60.

[12] Y.-I. Kim, P.M. Woodward, K.Z. Baba-Kishi, C.W. Tai, Characterization of the structural, optical, and dielectric properties of oxynitride perovskites AMO_2N (A= Ba, Sr, Ca; M= Ta, Nb), Chem. mater. 16 (2004) 1267-1276.

[13] D. Chen, D. Habu, Y. Masubuchi, S. Torii, T. Kamiyama, S. Kikkawa, Partial nitrogen loss in $SrTaO_2N$ and $LaTiO_2N$ oxynitride perovskites, Solid State Sci. 54 (2016) 2-6.

[14] A. Hosono, R.P. Stoffel, Y. Masubuchi, R. Dronskowski, S. Kikkawa, Melting behavior of alkaline-earth metal carbodiimides and their thermochemistry from first-principles, Inorg. Chem. 58 (2019) 16752-16760.

[15] T. Takeda, N. Hatta, S. Kikkawa, Ammonia nitridation synthesis and structural change of strontium cyanamide polymorphs, J. Ceram. Soc. Jpn. 115 (2007) 729-731.

[16] A. Perret, A.M. Krawezynski, Recherches sur les cyanamides métalliques, Helv. Chim. Acta 15 (1932) 1009-1022.

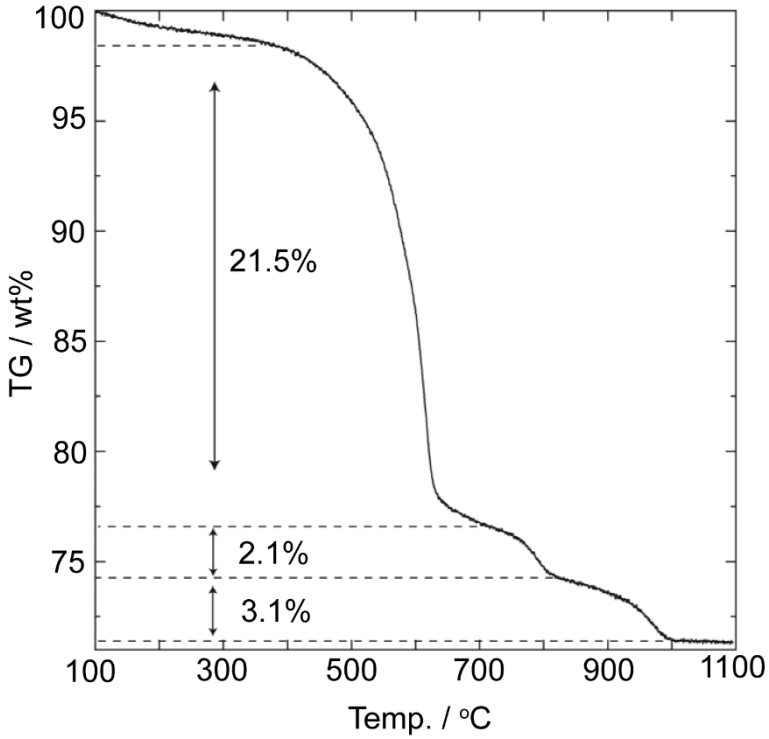

Figure 1. TGA curve obtained from a $Sr_2Nb_2O_7/C_3N_4$ mixture in a nitrogen flow.

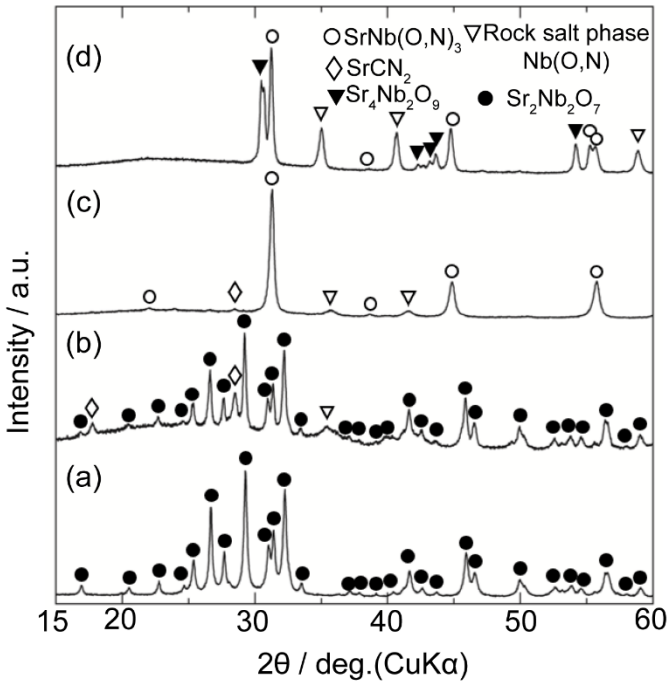

Figure 2. XRD patterns for (a) the starting oxide $Sr_2Nb_2O_7$ and the products after TGA trials with heating to (b) 700 °C, (c) 800 °C and (e) 1100 °C.

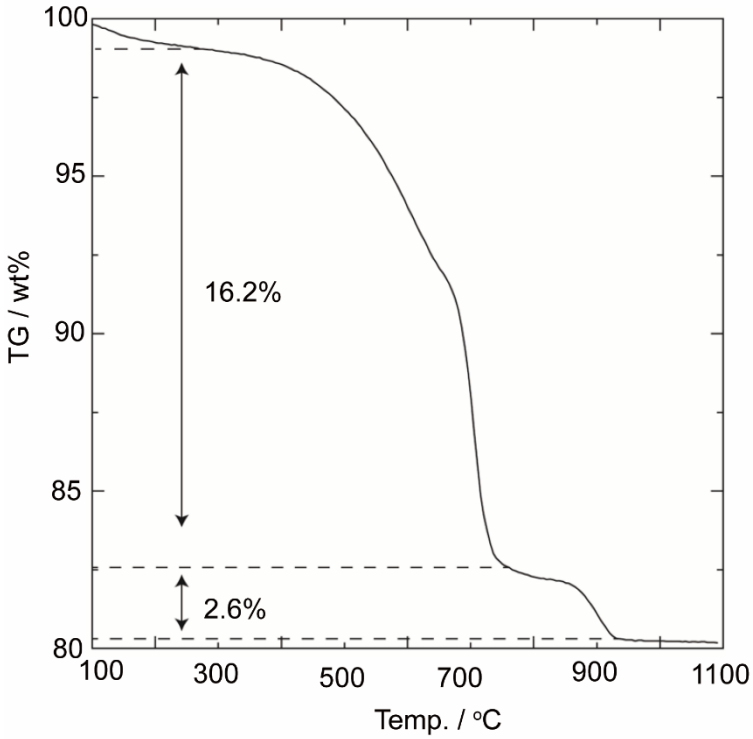

Figure 3. TGA curve obtained from $Ca_2Ta_2O_7/C_3N_4$ mixture under a nitrogen flow.

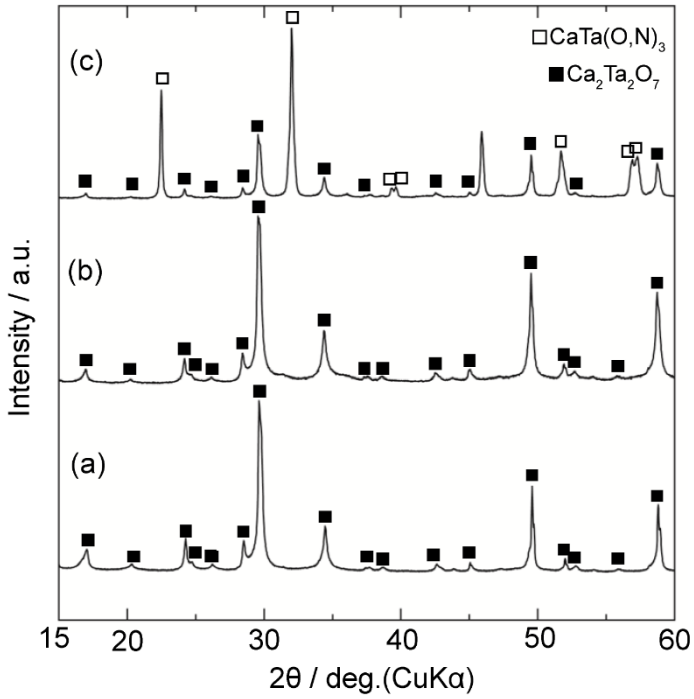

Figure 4. XRD patterns for (a) the starting oxide $Ca_2Ta_2O_7$ and the products after TGA trials with heating to (b) 750 °C and (c) 1100 °C.

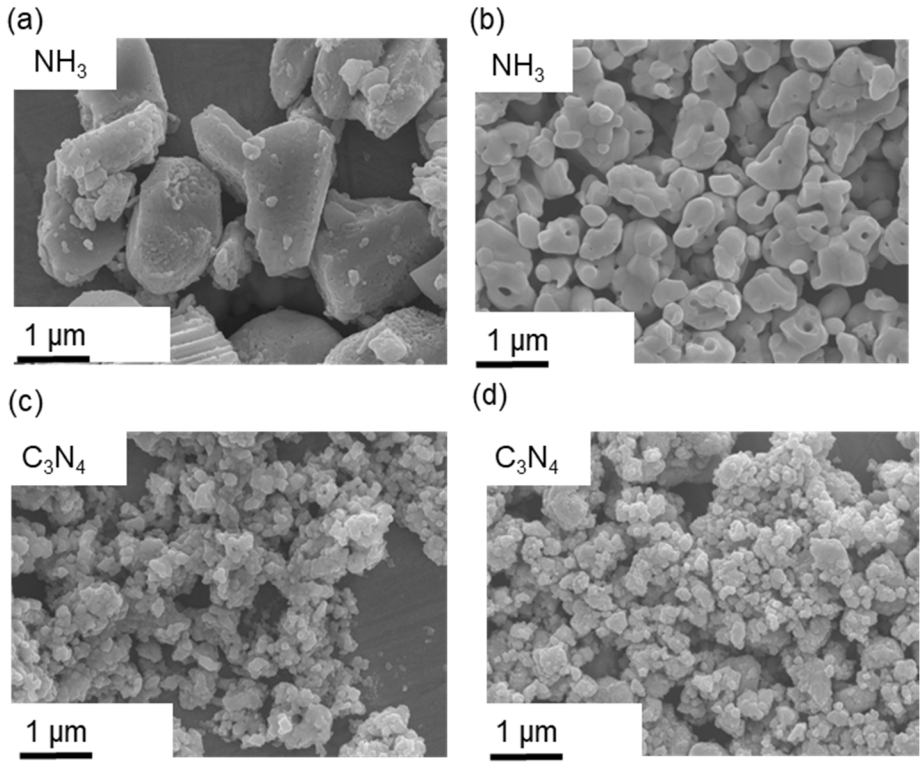

Figure 5. FE-SEM images of the oxynitrides (a and c) $SrNb(O,N)_3$ and (b and d) $CaTa(O,N)_3$ prepared using (a and b) ammonia (c and d) C_3N_4.